

Friedrich Pfeiffer

Energy considerations for frictional impacts

Received: 30 January 2009 / Accepted: 24 June 2009 / Published online: 6 November 2009
© Springer-Verlag 2009

Abstract Many machine and mechanism processes are accompanied by impacts with friction. They arise by short-time contacts between two or more bodies, and they generate energy losses mainly due to friction in tangential contact directions. During the last two decades, a couple of impact models based on the theory of rigid body contact were established connected with the names of Moreau, Frémond, and Glocker, which all work quite satisfactorily with respect to practical applications, although some examples indicate deviations requiring more investigations with respect to the impact models and the type of examples considered. We shall focus on Glocker's model, for which some experimental verifications are available by Beitelshmidt. A missing link are energy considerations, which are available, but nevertheless do not provide us with a complete information for all possible cases. The paper tries to fill a bit this gap by founding the investigations on a combined phenomenological and theoretical basis.

Keywords Impacts with friction · Non-smooth mechanics · Energy losses · Impact structure

1 Introduction

We consider rigid bodies as part of a multibody system, which come into contact including normal and tangential features, and we focus especially on short-time contacts and the energy losses accompanying such processes. The principal situation is illustrated in Fig. 1. Starting with the models as developed in [1,3,7,9], we use the following classical assumption for impacts with and without friction:

- The duration of the impact is so short, that the mathematical description may assume a zero impact time.
- As a consequence wave processes, which would take place in a finite time interval, will be neglected. Important indicators are the impact time in comparison to the wave propagation time, wave reflection and dispersion. In many technical problems, such as wave phenomena do not play a role.
- Following these assumptions, the mass distribution of the body is considered to be constant during the impact, the bodies remain rigid, or globally elastic.
- All positions and orientations of the impacting bodies remain constant during the time of impact. The translational and rotational velocities of the bodies are finite and may change jerky during the impact.
- Accordingly, the position of the impact point and that of the normal and tangential vectors remain constant.
- All forces and torques, which are not impulsive forces and torques, remain also constant during the impact.
- All impulses evolving during the impact act in a constant direction. Their lines of action do not change and correspond to the normal and tangential vectors in the impact point.

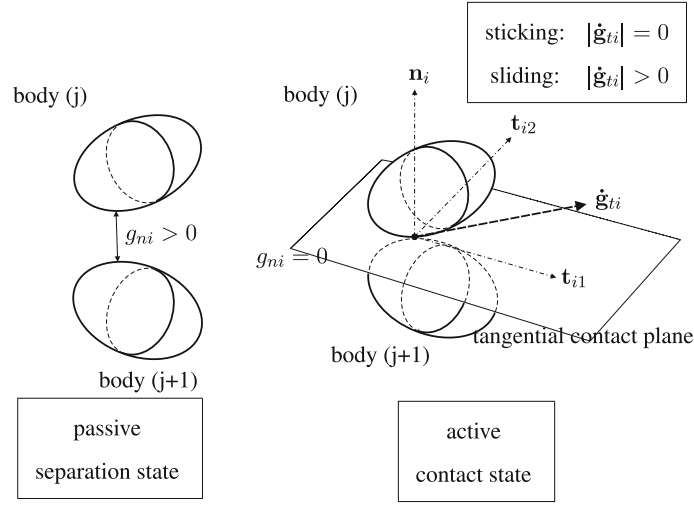


Fig. 1 Principal situation in a multibody contact (i)

- The impact can be divided into two phases: the compression phase and the expansion phase.
- The compression phase starts at time t_A and ends at time t_C . The end of the compression equals the start of the expansion phase. Expansion is finished at time t_E , which is also the end of the impact.

During compression impulses in normal and tangential directions of the contact are stored, and during expansion, these stored impulses are released, both processes accompanied by losses. The losses are described by Poisson's friction law. A detailed description of these processes may be found in the literature [3–5, 9] with increasing depth of mathematical representation.

2 Impact characteristics

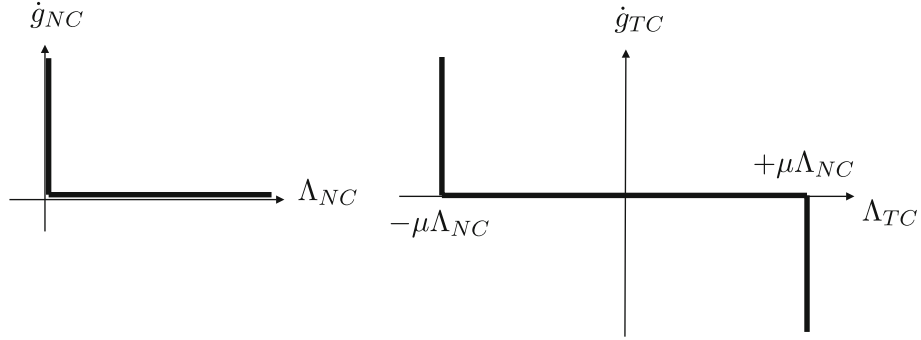
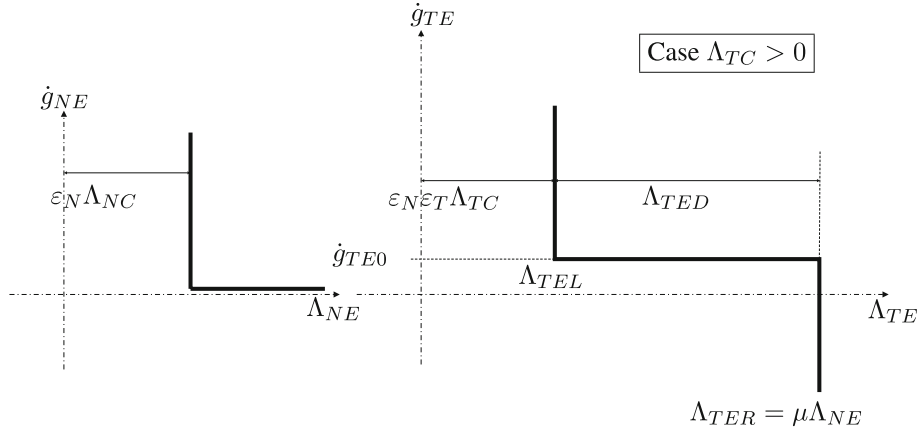
According to Moreau [5, 6], we may express the dynamics with and without impacts by one measure differential equation in the form

$$\mathbf{M}d\mathbf{u} + \mathbf{h}dt - \mathbf{W}d\boldsymbol{\lambda} = \mathbf{0} \iff \begin{cases} \mathbf{M}\dot{\mathbf{u}} + \mathbf{h} - \mathbf{W}\boldsymbol{\lambda} = \mathbf{0} & (t \neq t_i) \\ \mathbf{M}(\mathbf{u}^+ - \mathbf{u}^-) - \mathbf{W}\boldsymbol{\Lambda} = \mathbf{0} & (t = t_i) \end{cases} \quad (1)$$

The term $\mathbf{W}\boldsymbol{\lambda}$ contains all contact reactions due to non-impulsive contacts and the term $\mathbf{W}\boldsymbol{\Lambda}$ all impulsive contact reactions. The time $t_i \in I_{kl}$ represents one of the instants (i), where an impact takes place. The vector \mathbf{h} includes all non-impulsive and applied forces, whatsoever, and for multibody systems without closed loops we also include in the generalized coordinates $(\mathbf{q}, \dot{\mathbf{q}})$ all bilateral constraints.

We start with the compression phase and the normal impact direction. At the end of compression the relative normal velocity is zero, $\dot{g}_{Ni} = 0$. The tangential compression phase is characterized mainly by friction. At the end of compression, we may have three states: first, sliding in a positive tangential direction ($\dot{g}_{TC} > 0$), where the tangential impulse acts during this phase in opposite direction with $\boldsymbol{\Lambda}_{TC} = -\mu\boldsymbol{\Lambda}_{NC}$, second, sticking at the end of compression ($\dot{g}_{TC} = 0$), where the tangential impulse is small enough to generate sticking during the whole compression phase, and third, sliding in a negative tangential direction ($\dot{g}_{TC} < 0$), where the tangential impulse acts during this phase in opposite direction with $\boldsymbol{\Lambda}_{TC} = +\mu\boldsymbol{\Lambda}_{NC}$. The processes for these two directions are depicted by the well-known graphs of Fig. 2.

The impulse stored during compression is released with a loss governed by Poisson's law. Restoring the tangential impulse affords some additional considerations. According to Poisson's law, we get back the stored tangential impulse $\boldsymbol{\Lambda}_{TCi}$ of the (i)th contact with a certain loss, that is $(\varepsilon_{Ti}\boldsymbol{\Lambda}_{TCi})$, where Poisson's losses are quantified by $(0 \leq \varepsilon_{Ti} \leq 1)$. The tangential friction coefficient ε_{Ti} must be measured. But this contains not all losses during expansion. The restoration of the tangential impulse possesses another quality compared with the restoration of the normal impulse, because it cannot take place independently from the normal impulse, which as a matter of fact represents the driving constraint impulse for the generation of tangential friction


Fig. 2 Contact laws for impacts

Fig. 3 Shifted normal and tangential characteristics for impact expansion

forces. Therefore, we shall assume, that the restoration of the tangential impulse is additionally accompanied by losses in “normal direction” expressed by ϵ_{Ni} . Figure 3 illustrates these processes, see also [3, 7].

Some remarks concerning “stored impulses” might be necessary at this point. The “exact” physical process of contacting bodies consists of some local elastic deformations within and around the contact zone in both directions, normal, and tangential. In addition, frictional forces develop between the contacting surfaces. Deformation energy is stored and then again released with losses. Therefore and strictly speaking, we store and release elastic energy. On the other hand, we do not model that process. We assume rigid body contacts and represent the individual contact motion by differential equations of first order and not of second order, which means, we are describing the dynamics in terms of velocities and impulses and not in terms of accelerations and forces. The storage of impulses, which is also formally necessary within the framework of the rigid body model, cannot be explained simply and in a physical way, but it makes sense and is consistent from the standpoint of rigid body modeling.

3 Energy losses

The loss of energy is the difference of the total system energy after an impact and before an impact. In terms of the generalized velocities $\dot{\mathbf{q}}$, we write [7]

$$\begin{aligned} \Delta T &= T_E - T_A \leq 0 \\ \Delta T &= \frac{1}{2} \dot{\mathbf{q}}_E^T \mathbf{M} \dot{\mathbf{q}}_E - \frac{1}{2} \dot{\mathbf{q}}_A^T \mathbf{M} \dot{\mathbf{q}}_A = \frac{1}{2} (\dot{\mathbf{q}}_E + \dot{\mathbf{q}}_A)^T \mathbf{M} (\dot{\mathbf{q}}_E - \dot{\mathbf{q}}_A). \end{aligned} \quad (2)$$

These are expressions considering scleronomic systems without an excitation by external kinematical sources. Applying the relations as presented in [9], we get for the energy expression in the form

$$\begin{aligned}
2\Delta T &= 2\Delta T_1 + \Delta T_2 = +2 \begin{pmatrix} \dot{\mathbf{g}}_{NE} \\ \dot{\mathbf{g}}_{TE} \end{pmatrix}^T \left[\begin{pmatrix} \Lambda_{NC} \\ \Lambda_{TC} \end{pmatrix} + \begin{pmatrix} \Lambda_{NE} \\ \Lambda_{TE} \end{pmatrix} \right] \\
&\quad - \left[\begin{pmatrix} \Lambda_{NC} \\ \Lambda_{TC} \end{pmatrix} + \begin{pmatrix} \Lambda_{NE} \\ \Lambda_{TE} \end{pmatrix} \right]^T \mathbf{G} \left[\begin{pmatrix} \Lambda_{NC} \\ \Lambda_{TC} \end{pmatrix} + \begin{pmatrix} \Lambda_{NE} \\ \Lambda_{TE} \end{pmatrix} \right] \\
\text{with } \mathbf{G} &= \begin{pmatrix} \mathbf{G}_{NN} & \mathbf{G}_{NT} \\ \mathbf{G}_{TN} & \mathbf{G}_{TT} \end{pmatrix} \quad \text{where } \mathbf{G}_{ij} = \mathbf{W}_i^T \mathbf{M}^{-1} \mathbf{W}_j, \quad i, j \in \{N, T\}
\end{aligned} \tag{3}$$

\mathbf{G} is the mass projection matrix, which is quadratic and positive definite with the exception of dependent constraints, where it is semidefinite. The $\dot{\mathbf{g}}$ are relative contact velocities and the Λ impulses. The indices N, T stand for normal and tangential direction, respectively, the indices C, E for the end of compression and the end of expansion, respectively. The second term of the energy equation is a quadratic form and always positive or zero, and from this we have $\Delta T_2 \leq 0$, always. The energy loss has to be negative, which will be decided by the first term of the above relations. If this term is negative or at least zero, the condition $\Delta T \leq 0$ will hold. Therefore, we shall concentrate on the first term which writes in more detail

$$\begin{aligned}
2\Delta T_1 &= +2 \begin{pmatrix} \dot{\mathbf{g}}_{NE} \\ \dot{\mathbf{g}}_{TE} \end{pmatrix}^T \left[\begin{pmatrix} \Lambda_{NC} \\ \Lambda_{TC} \end{pmatrix} + \begin{pmatrix} \Lambda_{NE} \\ \Lambda_{TE} \end{pmatrix} \right] \\
&= 2[\dot{\mathbf{g}}_{NE}^T (\Lambda_{NC} + \Lambda_{NE}) + \dot{\mathbf{g}}_{TE}^T (\Lambda_{TC} + \Lambda_{TE})]
\end{aligned} \tag{4}$$

For the evaluation of this equation, we have to discuss the models. The compression/expansion model as considered here is a very powerful one providing us with the necessary informations for impulsive processes in multibody systems, but it does not provide us with the details within the compression and expansion phases necessary for energy considerations. We get informations at three points A, C, E (A=beginning, C=end compression, E=end expansion), but not between these points.

We know for example, that for an impact with sliding or sticking the relative normal distance and velocity have to be zero. Otherwise, we do not get tangential impact and contact motion. But on the other hand, the results for the points A, C, E would give us for E only a non-zero normal velocity, which appears in physical reality only at the very end of the impact and not during expansion. To solve this problem without disturbing the model concept, it is sufficient to define the transition locations at the very end of the compression phase (transition (C/E)) and of the expansion phase (point E). Such transitions from sticking to sliding or vice versa and from contact to detachment are assumed to take place in an infinitesimal short time with no energy effects.

So it can be shown, that the first term $\dot{\mathbf{g}}_{NE}^T (\Lambda_{NC} + \Lambda_{NE})$ of the energy equation (4), last line, is not zero due to positive normal impulses $(\Lambda_{NC} + \Lambda_{NE})$ and due to a non-zero end velocity $\dot{\mathbf{g}}_{NE}$ after the impact, which is physically reasonable for a separation of the two contacting bodies. But on the other hand, sliding or sticking during expansion requires a zero normal relative velocity $\dot{\mathbf{g}}_{NE}$ in the contact, which makes the above-mentioned term to zero. The Λ_{NE} -value slips into the corner of Fig. 3 allowing the system to build up the necessary separation velocity. From this we assume, that during the expansion phase the term $\dot{\mathbf{g}}_{NE}^T (\Lambda_{NC} + \Lambda_{NE}) = 0$ is zero.

As a result of these arguments and of the last condition of continual contact during the impact we get for compression and expansion $\Lambda_N > 0$ and $\dot{\mathbf{g}}_N = 0$, which is also part of the complementarity, and therefore simply

$$2\Delta T_1 = 2\dot{\mathbf{g}}_{TE}^T (\Lambda_{TC} + \Lambda_{TE}), \tag{5}$$

the sign of which we have to investigate. For this purpose, we consider this equation with respect to the following four cases, see for the arguments always the Figs. 2 and 3:

- **sticking during compression, sticking during expansion**

The tangential impulses have to be within the appropriate friction cones. The tangential velocities are zero, therefore, we need not to consider the magnitudes of the impulses.

$$\begin{aligned}
-\text{diag}(\mu_0)\Lambda_{NC} &\leq \Lambda_{TC} \leq +\text{diag}(\mu_0)\Lambda_{NC}, \quad \Lambda_{TEL} \leq \Lambda_{TE} \leq \Lambda_{TER} \\
\implies \dot{\mathbf{g}}_{TE}^T (\Lambda_{TC} + \Lambda_{TE}) &= 0
\end{aligned}$$

- **sliding during compression, sliding during expansion**

Sliding means single-valued impulse laws according to Coulomb's law. Some difficulties will appear for the cases with reversed sliding, that means, with a tangential relative velocity the sign of which is different during compression and during expansion. Therefore, we have to consider the two cases without and with tangential reversibility. For the first case, we do not have a change of sign of the relative tangential velocity, which gives $\text{sign}(\dot{\mathbf{g}}_{TC}) = \text{sign}(\dot{\mathbf{g}}_{TE})$. This comes out with the relations:

$$\begin{aligned}\dot{\mathbf{g}}_{TE}^T \Lambda_{TC} &= -\dot{\mathbf{g}}_{TE}^T [\text{diag}(\mu) \text{sign}(\dot{\mathbf{g}}_{TE}) \Lambda_{NC}] = -\text{diag}(\mu) |\dot{\mathbf{g}}_{TE}| \Lambda_{NC} \leq \mathbf{0}, \\ \implies \dot{\mathbf{g}}_{TE}^T (\Lambda_{TC} + \Lambda_{TE}) &< 0\end{aligned}$$

The case with tangential reversibility is more complicated, because it includes a change of sign of the tangential relative velocity and thus at least an extremely short stiction phase, which we put exactly at the point (end of compression)/(beginning of expansion). The sliding velocity during compression decreases until it arrives at one of the corners of Fig. 2, then we get an extremely short shift from this corner to the other one, which allows the contact to build up a tangential velocity with an opposite sign, then valid for the expansion phase. Only by such a short stiction phase, a reversal of tangential velocity is possible. On the other hand, such a transition from stick to slip, as short as it might be, follows the same process as for the next case sticking/sliding. Therefore, it is dissipative:

$$\implies \dot{\mathbf{g}}_{TE}^T (\Lambda_{TC} + \Lambda_{TE}) < 0$$

- **sticking during compression, sliding during expansion**

The transition from sticking in compression and sliding in expansion follows the mechanism (Fig. 2): if $\Lambda_{TC} \geq \mathbf{0}$, then sliding is only possible for being at the very end of compression on the friction cone boundary with $\Lambda_{TC} = \pm \text{diag}(\mu) \Lambda_{NC}$ and $\dot{\mathbf{g}}_{TC-at} \leq \mathbf{0}$ (at = after transition stick-slip). This results always in a negative sign of the expression ($\dot{\mathbf{g}}_{TE}^T \Lambda_{TC}$). For the rest, we assume a continuation of the signs after going from stick to slip [$\text{sign}(\dot{\mathbf{g}}_{TE}) = \text{sign}(\dot{\mathbf{g}}_{TC-at})$]. Then, we arrive at:

$$\implies \dot{\mathbf{g}}_{TE}^T (\Lambda_{TC} + \Lambda_{TE}) < 0$$

- **sliding during compression, sticking during expansion**

This case is again simpler, because we get sticking at the end with a zero relative tangential velocity. Therefore, we need not to consider the impulses.

$$\implies \dot{\mathbf{g}}_{TE}^T (\Lambda_{TC} + \Lambda_{TE}) = 0$$

- **summarized result for all cases**

$$\implies \dot{\mathbf{g}}_{TE}^T (\Lambda_{TC} + \Lambda_{TE}) \leq 0 \implies \Delta T_1 \leq 0 \implies \Delta T \leq 0$$

One may object that the above considerations assume in the case of multiple impacts, the same impact structure for all simultaneously appearing impacts, which is usually not true. But even any combination of the above four cases for simultaneous impacts gives a loss of energy. Practical experience indicates in addition that the simultaneous appearance of impacts is extremely scarce, it is an event, which nearly does not happen.

As a final result, we may state that the above evaluation confirms the physical argument, that any impact processes are accompanied by energy losses. This confirms also the well-known statement of Carnot, that “*in the absence of impressed impulses, the sudden introduction of stationary and persistent constraints that change some velocity reduces the kinetic energy. Hence, by the collision of inelastic bodies, some kinetic energy is always lost*”.

The above considerations and the underlying theory have been confirmed by the experimental work of Beitelschmidt [1]. In addition, its validity could be observed by many industrial projects where the non-smooth methods were applied [2, 10]. As a “pars pro toto”—presentation we shall have a closer look to Beitelschmidt's measurements, because first and according to my knowledge these are the first carefully performed and unambiguous tests of that field, and second, these measurements illustrate in a clear way the losses of impacts with friction, though not directly but through the relationship of incoming and outgoing velocities.

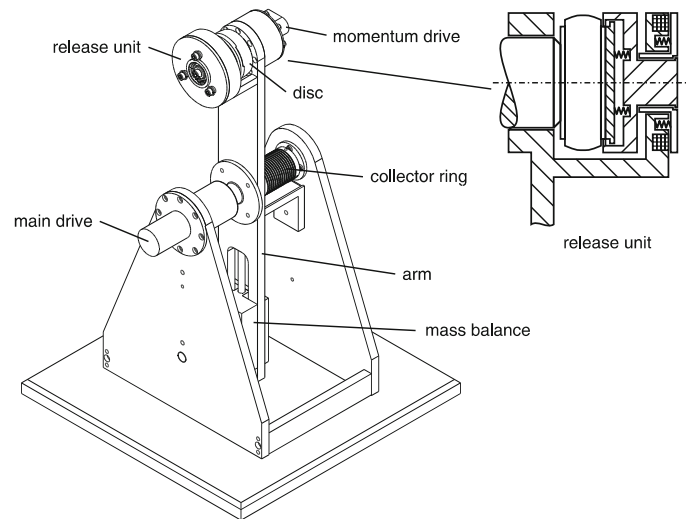


Fig. 4 Throwing machine

4 Experimental verification

4.1 The test set-up

In designing a test set-up for measuring impacts with friction a first principal decision with respect to the experiments for the geometrical type of impact, plane or spatial, had to be made. Colliding bodies moving in a plane are connected with linear complementarity problems, spatial contacts generate nonlinear complementarities. Therefore, motion in a plane was considered where one body is a disc and the other one the ground. On this basis, some further requirements and performance criteria were defined as follows:

- maximum translational velocity (10 m/s)
- maximum rotational velocity (40 rps)
- throw direction ($0^\circ - 90^\circ$)
- release time (< 12 ms)
- encoder main axis (1600 points)
- encoder momentum axis (400 points)
- throwing disc (diameter 50 mm, thickness 20 mm, weight 300 g)
- continuous variable velocity control
- translation and rotation decoupled
- disturbance-free support and release of disc
- mass balance, statically and dynamically
- electric drives (pulse width modulation with 250 steps)
- automatic control for the throwing process, the release of stroboscope and camera

As a result, the machine of Fig. 4 was designed and built, which met all requirements. A release unit containing the disc is mounted at the end of a rotating arm with mass balance. The unit itself drives the disc giving it a prescribed rotational velocity. Main drive and momentum drive are decoupled allowing to control the two speeds independently. The rotation of the arm generates a translation, the rotation of the release unit a rotation of the disc, with reference to the disc at the time instant of release. The flight of the body is photographed under stroboscopic exposure in a dark room before and after hitting his target. From the evaluation of the photographs, one can calculate the velocities and the position of the body immediately before and after the impact.

Figure 5 depicts the structure of the test set-up. A computer performs all control calculations, processes sensor data, evaluates control torques, releases stroboscope and camera, and records all measured data. Within this overall structure, we find for each drive an individual control concept, which has thoroughly been optimized with regard to the above requirements [1]. In addition, a typical sequence of events for the test procedure is depicted in Fig. 6, where the central processor works with a frequency of 250 Hz.

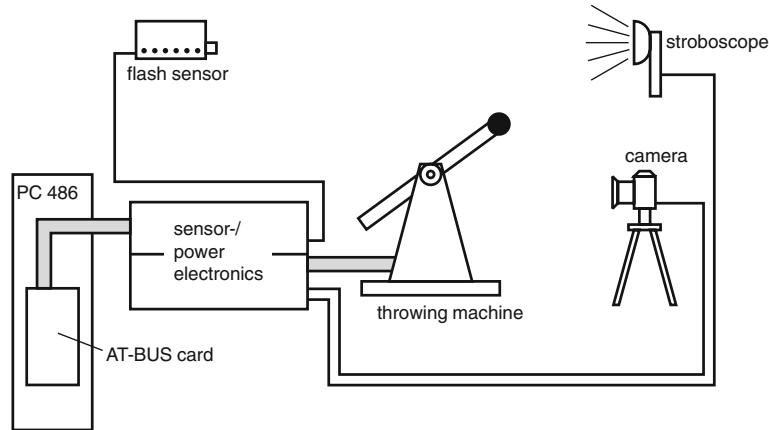


Fig. 5 Structure of the complete test set-up

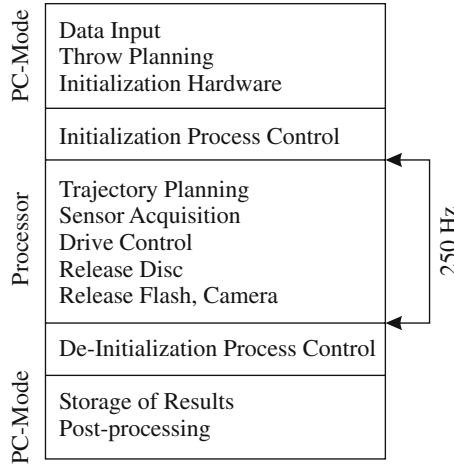


Fig. 6 Sequence of test events

All computer codes have been realized in C++, which was feasible due to the fact that the PC-Mode activities are not critical with respect to time.

4.2 Results

The evaluation of the measurements as recorded by the camera and the processor was straightforward. Figure 7 illustrates the method and includes additionally two photographs of experiments. Especially, the rubber disc experiment shows nicely a reversal of the trajectory due to the disc's rotation. The experimental process provided thus a very precise and well reproducible basis for determining the properties of impacts with friction.

In the following, we shall give only a few examples out of more than 600 experiments performed with axisymmetric and with eccentric discs. In all cases, the comparisons with theory are good to excellent [1]. In the following diagrams, we shall use dimensionless velocities and impulses defined by

$$\begin{aligned}
 \gamma &= \frac{\dot{g}_{TA}}{-\dot{g}_{NA}}, & \gamma_{NC} &= \frac{\dot{g}_{NC}}{-\dot{g}_{NA}}, & \gamma_{TC} &= \frac{\dot{g}_{TC}}{-\dot{g}_{NA}}, \\
 \gamma_{NE} &= \frac{\dot{g}_{NE}}{-\dot{g}_{NA}}, & \gamma_{TE} &= \frac{\dot{g}_{TE}}{-\dot{g}_{NA}}, & \gamma_{TE0} &= \frac{\dot{g}_{TE0}}{-\dot{g}_{NA}},
 \end{aligned} \tag{6}$$

where the indices N , T refer to normal and tangential directions. The indices A , C , E are the beginning and the end of the compression phase, and the end of the expansion phase, respectively. The kinematical magnitude

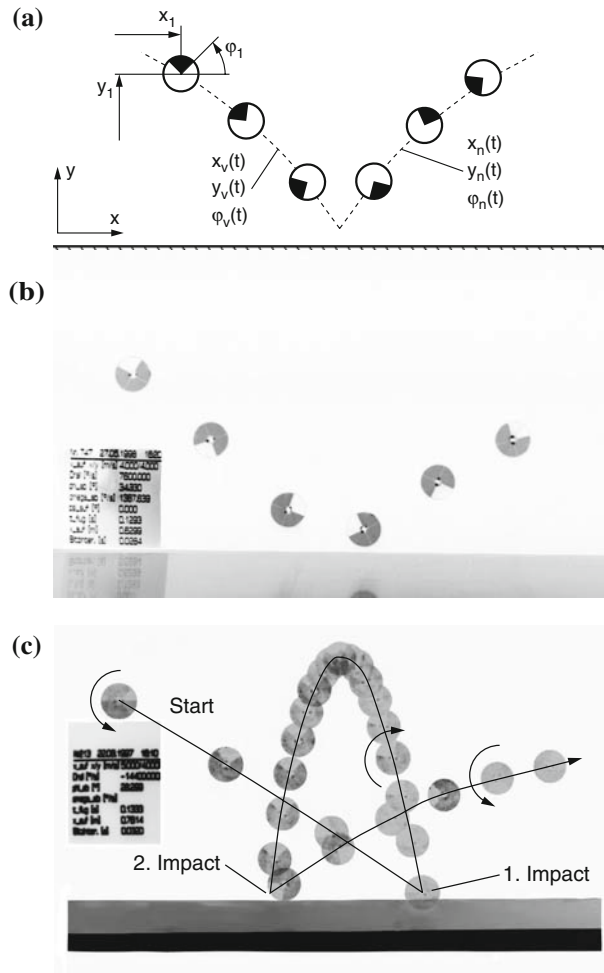


Fig. 7 Disc trajectory during an experiment, **a** method of evaluation, **b** photograph steel, **c** photograph rubber

\dot{g} is a relative velocity in the contact zone. Experiments usually generate a negative normal velocity ($-\dot{g}_{NA}$) at the beginning.

Figure 7 indicates the evaluation process for all experimental results. For every small part of the trajectory, we perform three stroboscope flashes thus achieving a certain redundancy for the measurements. The trajectory is a parabola, and the velocity possesses a positive component in x - and a negative component in y -direction. The stroboscopic measurements in connection with the marked sectors of the discs allow a safe evaluation of the translational and rotational velocities of the discs. To find the time and the point of impact, the measurements before and after such an impact are represented by a statistical interpolation scheme, which allows to determine the impact together with the dispersion of the results.

Figure 7 gives two examples. The picture of Fig. 7b shows a steel disc approaching the ground with a translational and rotational velocity and leaving the ground with more or less a similar trajectory.

Figure 7c represents more spectacular results. The rubber disc appears from the left side with a horizontal velocity of 5 m/s and a vertical velocity of 4 m/s in negative y -direction. The rotational velocity in a counter-clockwise direction amounts to 40 rps (2400 rpm). This results in a tangential relative velocity of 12.5 m/s at the point of impact. After the first contact, the velocities reverse by the impact jump, and the disc flies backwards with a clockwise rotation. At the second impact, the velocities change again, and the disc flies forward with the original direction of rotation.

As a result we may state, that for the rubber case the impact coefficient of restitution in normal direction depends much more on the velocities at collision than for stiff materials, that we get a typical characteristic behavior in the sense of tangential reversibility, and that for soft materials like rubber, we may have friction

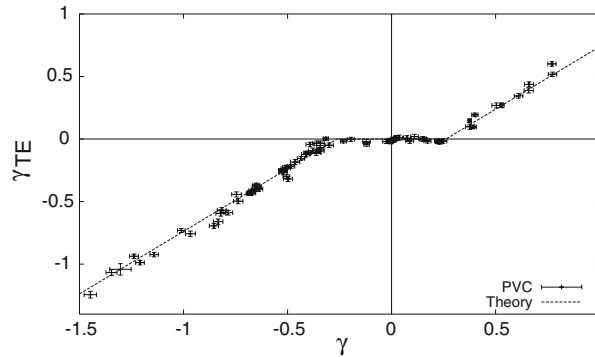


Fig. 8 Dimensionless tangential relative velocity after versus before the impact, PVC-body

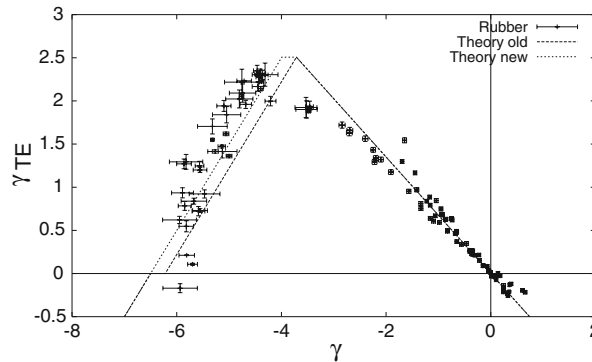


Fig. 9 Dimensionless tangential relative velocity after versus before the impact, rubber-body

coefficients larger than one ($\mu > 1$). The theory describes this behavior very well, where especially for soft materials a correction is advantageous (see below).

Figure 8 shows results of experiments with the PVC test body. The experiments are marked by crosses, the dotted line shows the theoretical result. For small tangential relative velocities before the impact, sticking occurs, and the rolling constraint between disc and ground is fulfilled after the impact. If the relative velocity is big enough, the body slides throughout the impact and has a reduced tangential relative velocity at the end of the impact. No tangential reversion occurs.

A similar diagram for a rubber-body is shown in Fig. 9. For most of the impacts, the tangential relative velocity has changed during the impact: the bodies collide with a negative relative velocity and separate with a positive velocity. The inclination of the line through the origin is $-\varepsilon_N \varepsilon_T$. If ε_N is known from another simple experiment, one can evaluate the coefficient of tangential reversibility from this plot. For this series of experiments, the parameters $\varepsilon_N = 0.75$ and $\varepsilon_T = 0.9$ were identified.

If the tangential relative velocity increases further, sliding occurs in the contact point during the impact. Then it is not possible to restore the elastic potential energy during the phase of expansion. For very high velocities, the rubber body slides during the whole impact and the effect of tangential reversibility is not longer visible. In Fig. 9, two lines are plotted, comparing theory with experiment. The new theory includes a correction with respect to Glocker's theory [3].

This correction can be explained by the difference of the contact point with Coulomb's friction and that point, where the resulting force due to local elastic deformations applies. In spite of the fact, that we do not model elasticity, we have to consider its effects also in a rigid body model. The difference of these points might generate an additional relative motion, which becomes large for highly elastic bodies like rubber. This gives a modification of the complementarities with respect to the friction cone, and thus a modification of the final results [1].

Summarizing these measurements we state, that the rigid body concept for impacts with friction according to Moreau and Glocker [3,6] are fully verified by extensive measurements. The correction as introduced by Beitelshmidt [1] are important for soft materials but have only minor influence for hard materials like steel or other metals. Furthermore all results indicate clearly some energy loss during the impact, expressed by smaller

output velocities at the end of expansion in comparison to the input velocities at the beginning of an impact. As all experimental and theoretical results coincide very nicely, we have thus a proof that the above energy considerations come out with the correct findings.

5 Conclusions

We consider impacts with friction applying rigid body theory of contacts, which makes use of the complementarity idea. Energy losses can be derived by using these complementarities in connection with the sign-properties of velocities and impulses for the compression and the expansion phases of the impact. Results clearly indicate a loss of energy during such a collision. Confidence into these findings is improved by the discussion of measurements, which first compare excellently well with theory and which secondly show clearly a reduction of energy during the impact by a significant reduction of the velocities after the collision in comparison with the incoming velocities.

References

1. Beitel Schmidt, M.: Reibstöße in Mehrkörpersystemen. Fortschritt-Berichte VDI, Reihe 11, Nr. 275, VDI-Verlag, Düsseldorf (1999)
2. Geier, T.: Dynamics of Push Belt CVTs. Fortschritt-Berichte VDI, Reihe 12, Nr. 654, VDI-Verlag, Düsseldorf (2007)
3. Glocker, C.: Dynamik von Starrkörpersystemen mit Reibung und Stößen. Fortschritt-Berichte VDI, Reihe 18, Nr. 182, VDI-Verlag, Düsseldorf (1995)
4. Glocker, C.: Set-Valued Force Laws—Dynamics of Non-Smooth Systems. Springer, Berlin (2001)
5. Leine, R., Nijmeijer, H.: Dynamics and Bifurcations of Non-Smooth Mechanical Systems. Springer, Berlin (2004)
6. Moreau J.J.: Unilateral contact and dry friction in finite freedom dynamics. In: Moreau, J.J., Panagiotopoulos, P.D. (eds.) International Centre for Mechanical Sciences, Courses and Lectures, vol. 302. Springer, Vienna (1988)
7. Pfeiffer, F.: Mechanical System Dynamics. Springer, Berlin (2008)
8. Pfeiffer, F.: Applications of unilateral multibody dynamics. Philos. Trans. R. Soc. **359**(1789), 2609–2628 (2001)
9. Pfeiffer, F., Glocker, Chr.: Multibody Dynamics with Unilateral Contacts. Wiley, New York (1996)
10. Sedlmayr, M.: Räumliche Dynamik von CVT-Keilkettengeräten. Fortschrittberichte VDI, Reihe 12, Nr. 558, VDI-Verlag, Düsseldorf (2003)